

**TECHNICAL NOTE****GENERAL; PATHOLOGY/BIOLOGY**

*Christian Jackowski,<sup>1,2,3</sup> M.D.; Marcel J. B. Warntjes,<sup>1,4</sup> Ph.D.; Johan Kihlberg,<sup>1</sup> R.N.; Johan Berge,<sup>3</sup> M.D.; Michael J. Thali,<sup>5</sup> M.D.; and Anders Persson,<sup>1</sup> M.D.*

## Quantitative MRI in Isotropic Spatial Resolution for Forensic Soft Tissue Documentation. Why and How?\*

**ABSTRACT:** A quantification of T1, T2, and PD in high isotropic resolution was performed on corpses. Isotropic and quantified postmortem magnetic resonance (IQpmMR) enables sophisticated 3D postprocessing, such as reformatting and volume rendering. The body tissues can be characterized by the combination of these three values. The values of T1, T2, and PD were given as coordinates in a T1–T2–PD space where similar tissue voxels formed clusters. Implementing in a volume rendering software enabled color encoding of specific tissues and pathologies in 3D models of the corpse similar to computed tomography, but with distinctively more powerful soft tissue discrimination. From IQpmMR data, any image plane at any contrast weighting may be calculated or 3D color-encoded volume rendering may be carried out. The introduced approach will enable future computer-aided diagnosis that, e.g., checks corpses for a hemorrhage distribution based on the knowledge of its T1–T2–PD vector behavior in a high spatial resolution.

**KEYWORDS:** forensic science, forensic radiology, postmortem imaging, postmortem MRI, quantitative MRI, whole-body MRI

Cross-sectional whole-body documentation using computed tomography (CT) is already used as an adjunct to autopsy examinations in several forensic institutes across Europe, North America, Japan, and Australia (1–3). The benefit of this pre-autopsy scanning is manifold. The corpse can be digitally “frozen” and the data can be consulted at any time again and as often as needed without destroying evidence (4). Furthermore, the three-dimensional (3D) data can be used for forensic reconstruction as they are always in scale (5). The advantage of fast data acquisition of CT technology allows whole-body scanning within minutes. Based on this 3D data, any desired cross-section at any window setting may be created and 3D volume rendering becomes possible (6). This provides the basis for so-called virtual CT data autopsies. CT is a powerful tool for visualization of gaseous (7), dental (6,8), skeletal (9), and foreign body findings (10,11) as well as for postmortem angiography (12,13). The major shortcoming of CT data is the rather insufficient soft tissue visualization, besides the lungs as one exception (3).

Postmortem magnetic resonance imaging (pmMRI) may close that important gap. Several pmMRI studies showed impressive soft tissue

visualization results compared to the autopsy appearance of the findings (14–18). In contrast to CT, being a whole-body documentation method with huge postprocessing potential, MRI remained, as yet, restricted to predefined cross-sections with predefined contrast weighting. In other words, the investigator has to decide, prior to scanning, the area to scan, the image plane orientation, and the contrast weighting to choose. As there are innumerable sequences, each providing different advantages for different pathologies, MRI suffers from the necessity to find a reasonable compromise between quality of the examination and the time spent. The result of these shortcomings is that MR scanning in general is limited to areas of interest and far from complete. The major disadvantage clearly is that the areas of interest need to be defined in advance. From the forensic point of view, a whole-body data set allowing any image plane at any contrast weighting to be calculated would fulfill the requirements of a forensic documentation. Each question could then be addressed with the optimal images generated in terms of location, plane orientation, and contrast weighting.

Furthermore, the 3D application of MR data for volume rendering was not possible in a satisfying manner. Clinical 3D applications were limited to contrast agent-enhanced data for vascular diagnostics only by using, for example, the maximum intensity projection technique to visualize the course of the examined vessel system. As the three-dimensionality of forensic findings cannot be ignored, pmMRI also suffered from the limitation to cross-sections.

In summary, there are four major requirements to be fulfilled by pmMRI in the future to catch up with postmortem CT in terms of feasibility of data acquisition/storage/usage to enhance forensic soft tissue documentation.

1. The MRI data need to be delivered in a reasonable 3D resolution, enabling reformatting of any section plane and volume rendering for visualization.

<sup>1</sup>Center for Medical Image Science and Visualization (CMIV), University Hospital, University of Linköping, SE-58185 Linköping, Sweden.

<sup>2</sup>Institute of Legal Medicine, University of Zürich, Winterthurerstrasse 190/52, 8057 Zürich, Switzerland.

<sup>3</sup>Department of Forensic Medicine, Artillerigatan 12, SE-58133 Linköping, Sweden.

<sup>4</sup>Division of Clinical Physiology, Department of Medicine and Care, University of Linköping, SE-58185 Linköping, Sweden.

<sup>5</sup>Institute of Forensic Medicine, University of Bern, Bülhlstrasse 20, 3012 Bern, Switzerland.

\*Supported by a grant of the Swedish Knowledge Foundation (KK-stiftelsen 2007/0170), a grant of the Swiss National Science Foundation (PBBE33-115060), and a grant of the Swedish National Board of Forensic Medicine (RMV) (all to Dr. Jackowski).

Received 14 Aug. 2009; and in revised form 20 Oct. 2009; accepted 31 Oct. 2009.

2. The MRI data need to be provided in a form that allows alteration of the image contrast weighting after scanning, enabling specifically addressed image processing and analysis for certain pathological and forensic questions.
3. The information about T1 and T2 relaxation times (In MRI the term “relaxation” describes the processes by which the nuclear magnetization prepared in a nonequilibrium state returns to the equilibrium distribution.) as well as the proton density (PD) should be used in a combined manner for specific tissue characterization, enabling color encoding of tissues and pathological alterations in volume rendering.
4. The entire body needs to be covered with the MRI examination.

If these four goals are fulfilled, a pmMRI data set of an entire human corpse can be stored that enables any specific question to be addressed afterward with optimal contrast weighting and optimal image plane direction at any body location. Also volume rendering will be possible allowing for MR data-based virtual autopsies of the soft tissues that were so far not sufficiently possible based on CT data with its rather poor soft tissue discrimination.

An MRI scanning technique for the future of pmMR scanning is presented that was developed to fulfill these four requirements.

## Material and Methods

For comprehensibility reasons, the main characteristics of the introduced scanning approach are dealt with separately throughout the publication although its combined application represents part of the fundamental progress. At this point, the authors assume that the interested reader has basic MR knowledge and only the information is given that is needed to understand the aspects of the newly implemented data acquisition approach. General MRI background information may be obtained from text books (19). MR scanning was performed on a 1.5 Tesla system (Achieva, Philips Medical Systems, Best, the Netherlands) using the Quadrature Body Coil and a 16 channel SENSE Neuro Vascular coil. All isotropic and quantified postmortem magnetic resonance (IQpmMR) examinations were performed with approval of the local ethics committee.

### Isotropic Multislice 3D Imaging

To be able to generate image planes after scanning differing from the original acquisition plane (as useful for cardiac imaging, where long and short axis images of the heart are visualized, for tracking gun shot channels or stab wounds or for imaging of the brain, where skull base parallel images are optimal), the acquired data should have isotropic voxel dimensions. This enables reformatting without loss of image quality. In general, MRI acquisitions are highly nonisotropic, i.e., slice thickness is substantially larger than the in-plane resolution. As an example, a field of view (FoV) of 300 mm using a  $400 \times 400$  pixel matrix results in a pixel size of 0.75 mm. Conventional MR slice thicknesses range between 3 and 10 mm, such that the resulting voxels have a length that is in order of 4–12 times its width. This approach increases the signal to noise ratio and reduces scan time for the clinical applications. However, to enable high-quality 3D postprocessing, such as reformatting or volume rendering, the dimension of the voxel should be similar for all three dimensions. That causes one minor shortcoming: the in-plane resolution will not be as high as theoretically possible in nonisotropic imaging. The presented technique is based on isotropic voxel dimensions of 1.2 mm (Fig. 1).

There are 3D sequences used in routine examinations. These acquire the 3D volume by performing a phase encoding in two

dimensions instead of generating thin slices with only one dimension to be phase encoded. Three-dimensional acquisitions are usually performed using short echo and repetition times because of the restrictions in available scan time. Therefore, these sequences are rather limited to T1 weighting and only of insufficient value for general forensic documentation purposes. Instead of performing a 3D acquisition, the newly introduced approach is based on a thin multislice acquisition that allows working with long repetition times. Until a full decay is reached, further slices are measured in the meantime. For the same reason, the multislice acquisition technique is also required for the quantification of the MR signal decays (see below).

### Quantifying the MR Signal Decay and Synthetic MR

Contrast in MRI images is manipulated with the MR scanner settings. Variations in the echo time (TE), repetition time (TR), and the application of preparatory pulses lead to so-called T1- or T2-weighted images. Usually a range of different settings are applied resulting in a set of images with various contrast weightings. However, the clinically optimized protocols do not provide the same image quality if applied in postmortem examinations. Corpses have a lower temperature than living patients, which alters their MRI characteristics, such as T1 and T2 relaxation. The pmMRI settings have to be optimized for all possible body core temperatures. A whole multiparameter investigation could be performed at any temperature to establish the optimal contrast for diagnosis. To avoid this time-demanding procedure in this work, a more direct approach was applied. A special sequence was performed that allows the simultaneous absolute measurement of T1 and T2 relaxation and PD. The quantification completely captures the information that is comparable to a whole range of contrast images (20,21).

To facilitate image interpretation, the quantification results can be visualized as conventional MRI images by means of the approach of synthetic MRI (SyMRI Brain Studio, SyntheticMR, Linköping, Sweden; Fig. 2). It is possible to calculate the expected image intensity of each pixel in the image as a function of TE, TR, and prepulses, based on the T1, T2, and PD maps. This way, any conventional T1-, T2-, and PD-weighted image can be synthesized using only a single quantification scan (20–24).

The advantage of such an approach is that the optimal scanner setting does not have to be known prior to the examination. Furthermore, the quantitative results will assist in the measurement of the absolute deviation from normal tissue.

### Tissue Characterization Based on a Combination of Quantified T1 and T2 Relaxation Times and PD

If the relaxation times and PD are known for every voxel, they can be displayed in a 3D coordinate system with R1 ( $1/T_1$ ), R2 ( $1/T_2$ ), and PD. Various tissues exhibit differences in one or several of those parameters and hence, each tissue is constituted of a cluster at a specific position in this 3D space. Unfortunately, there is no software today that can handle both the 3D real space and the 3D parameter space simultaneously. To circumvent this issue, one could choose to use only a single parameter, which can be handled by commercial CT software. A better approach is to define an axis through the 3D parameter space such that the projection onto this axis leads to an optimal discrimination of the various tissues. By using this approach, characteristic values are imposed on each tissue cluster. The optimal axis is similar to the Hounsfield Unit scale of CT data and the resulting images can be displayed

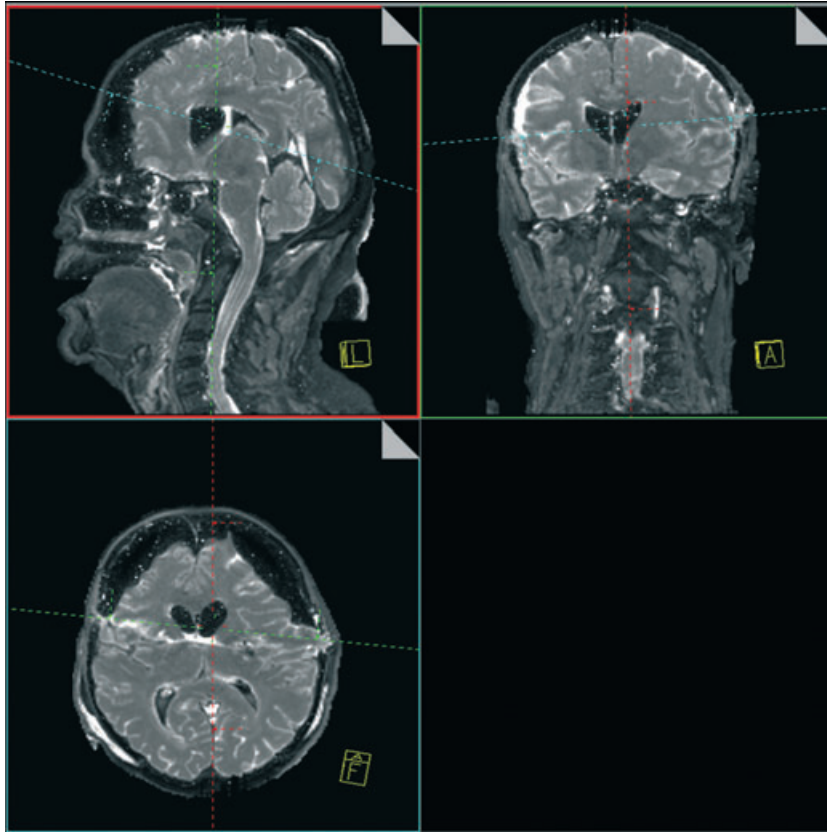


FIG. 1—Reformatting performed on a quantified isotropic postmortem magnetic resonance data set of the head (displayed in a predominant T2 weighting). Any wanted image plane can interactively be created in real time. Note the coloration of the lines and frames that indicate the relation of the different image planes to each other. The user can change the position of the lines as well as the angles and thereby generate any image plane from the acquired data, e.g., to examine the brain in 1.2-mm-thin slices and to adapt the slice orientation to a gun shot channel (lower left).

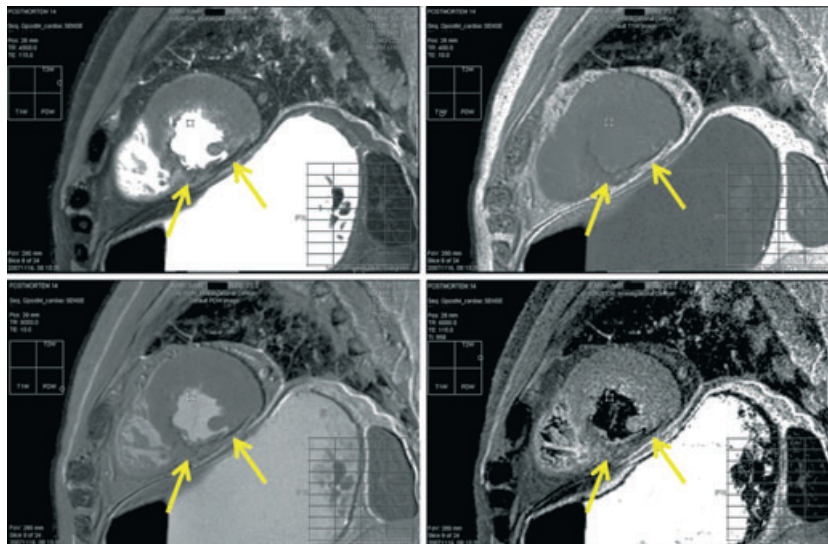


FIG. 2—Application of postmortem synthetic magnetic resonance (MR) in a case of chronic myocardial infarction. User interface of a recently implemented synthetic MR plug-in for Picture Archiving and Communication System work stations, which requires quantified MR data. After loading the data of a short axis image data set default settings for T1, T2, PD, and flair images are applied to start with. The user may choose any TE, TR, flip angle, or in case of inversion recovery sequences any inversion pulse delay for synthetic image reconstruction. Thereby, any noncontrast agent-enhanced image contrast weighting can be generated from the acquired data set. Note the severe shrinking of the inferior wall (arrows) with signal decrease in all four contrast weightings best visible in optimized T2 settings (upper left). T1-weighted upper right, PD-weighted lower left, and flair lower right. TR, repetition time; TE, echo time.

accordingly. Alternatively, the quantified parameters might be translated into a specific color scale, for example T1–T2–PD into red–green–blue. Using this approach, each tissue will have its own

unique color composition, which may assist in the visual recognition of the various tissue types. Quantification of MR signal decay in isotropic resolution allows color encoding of the tissues,

structures, and pathologies in combination within volume rendering, as is already possible for CT data. However, the soft tissue discrimination reaches new dimensions using MRI as input for the 3D visualization.

*Whole-body Imaging*

When the coverage of a large volume is required along the z-axis, as in coronal or sagittal images in whole-body scanning, there are several limitations to overcome. The acquisition FoV of an MRI scanner is determined by the homogeneity volume around the isocenter of the magnet. The diameter of this volume is in the order of 40–50 cm. To acquire images of the entire body length makes is necessary to move the corpse step by step through the scanner. Clinical MR scanning is normally an examination of a certain area, and the patient can be placed head first in the scanner when cranial imaging or imaging of the trunk is performed. However, when MR imaging of the legs or pelvic regions is needed, the patient would enter the scanner feet first. As postmortem whole corpse images are combined automatically according to their position within the 3D space, any movement and turning of the scanned object itself would result in insufficient image combination. This problem is solved by a sufficient table stroke, which allows scanning all levels from head to toe in the same direction. Practically, the device carries the corpse on the back side of the scanner when the body has entered the scanner head first and the feet have reached the center of the magnet.

After the actual acquisition, the images from the various stations must be merged into large images that cover the complete body. The two main challenges are to adjust the gray scaling of all images to a uniform appearance and the continuation of the data across the borders of neighboring stations.

The gray scaling of each image on every level is automatically optimized for the signal measured in that slice. Images of different body levels can cover distinctively differing volumes of body tissue. These differences in covered body tissue lead to partly differing gray scaling within the initial images. When interpreting single images, these differences have no relevance. However, when the

images are combined the slightly differing gray scaling becomes obvious at the border between the scan levels. This phenomenon was more apparent in T2-weighted scans (see Fig. 5c). The single images could have been manually corrected to better match in gray scaling. As this would be simply based on subjective impression of the investigator, we hesitated to do so in order to maintain the objectivity of the MR documentation. A possible future solution could be an automatic gray scaling based on the entire data of the corpse resulting in one homogenous MR image from head to toe.

The continuation of the resulting image across the scanning stations is sufficiently possible as long as there is no change of body position during scanning.

**Results**

*Isotropic Multislice 3D Imaging*

Figure 1 demonstrates the use of IQpmMR data for generation of reformatted images of a gun shot channel through the brain. Any image plane can be calculated interactively and in real time on a routinely used radiological workstation (example images: Leonardo, Siemens Medical, Syngo). No loss of image quality can be observed for any of the planes (acquisition plane was sagittal).

*Quantifying the MR Signal Decays and Synthetic MR*

Figure 2 shows a synthetically calculated set of short axis images with different contrast weightings of a chronic inferior myocardial infarction as the cause of death. The data set can be used to synthetically generate images simulating the settings that result in an optimal image contrast for a certain finding. Thereby, the data can be used to investigate the optimal scanning parameter settings for conventional MR scanning in case a certain finding needs to be documented in an even higher resolution than the introduced approach provides. Furthermore, it allows optimization of the parameter setting for the general postmortem use by investigating the relation between parameter setting and image contrast for certain findings at certain temperatures.

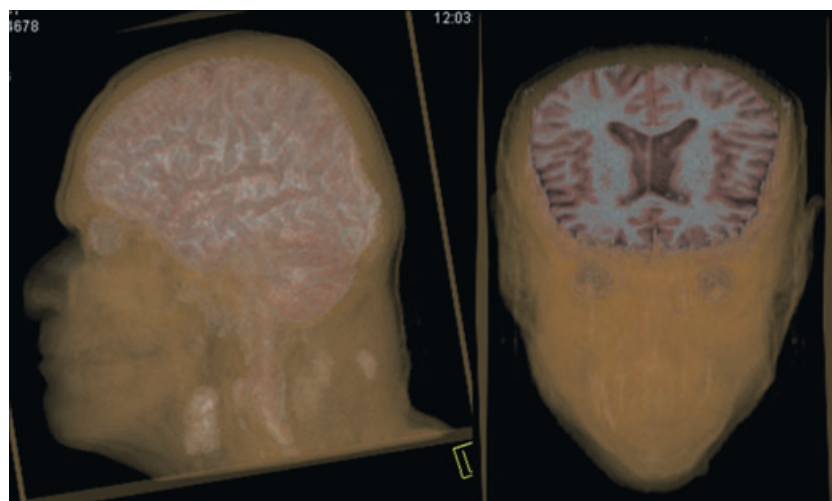


FIG. 3—Volume rendering based on postmortem quantified isotropic magnetic resonance (MR) data. The example shown demonstrates an approach to visualize the brain in its three-dimensional structure as well as its gray and white matter composition based on a certain vector visualization of the quantified MR data optimized for the central nervous system. Partly overlapping of brain tissues signal combinations with partial volume effect affected voxels along the air containing pharynx causes an enhancement of those too. The coloration of any other tissue becomes possible based on the combination of its quantified proton density as well as its T1 and T2 relaxation times.

*Tissue Characterization Based on a Combination of Quantified T1 and T2 Relaxation Times and PD*

Figures 3 and 4 show volume-rendered cranial data sets obtained with the introduced approach. Certain soft tissues or soft tissue findings can be visualized in their three-dimensionality. The first example aimed on visualization of the central nervous system and its composition of gray and white matter. Only the voxels

representing the values of either gray or white matter were given high opacity ramps. Further tissues have been combined in a low opacity ramp to outline basic anatomy.

Figure 4 shows a further example for the technique applied on a corpse with a gun shot wound to the head and consecutive fractures causing hematomas. In this visualization approach, a ramp for the central nervous system and another low opacity ramp combining further soft tissues are additionally included to display anatomic

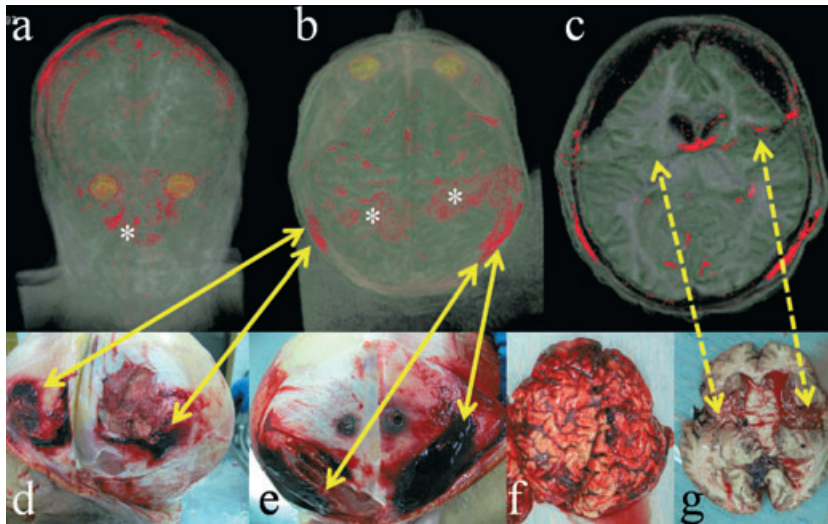


FIG. 4—Volume rendering based on postmortem quantified isotropic magnetic resonance data to visualize the three-dimensional hematoma distribution in a gun shot wound case. (a) AP view: Note a large subcutaneous right parietal hematoma as well as the subarachnoidal bleeding distribution. The specific relaxation behavior of vitreous fluid was given a yellow appearance to outline the eyeballs as anatomic fixed points in the data set. Further blood accumulations are present within the sinuses (asterisk). (b) Cranial view: Arrows indicate the correlation to the appending autopsy appearance of right and left parietal hematoma. Asterisks indicate subarachnoidal blood accumulations. (c) Cranial view on an axial slice along the gun shot channel. Note hemorrhages along the channel as well as brain tissue leaving the skull through the exit wound. Dashed arrows indicate the correlation to the appending autopsy appearance. (d) Left-sided exit wound with surrounding hematoma (small bone fragments removed). (e) Right-sided entrance wound with large dorsally oriented fracture hematoma. (f) Autopsy aspect of the brain with variable subarachnoidal hematoma. (g) Flechsig cut along the gun shot channel as autopsy correlation to panel c. Along the destruction zone, intra cerebral hemorrhages are present.

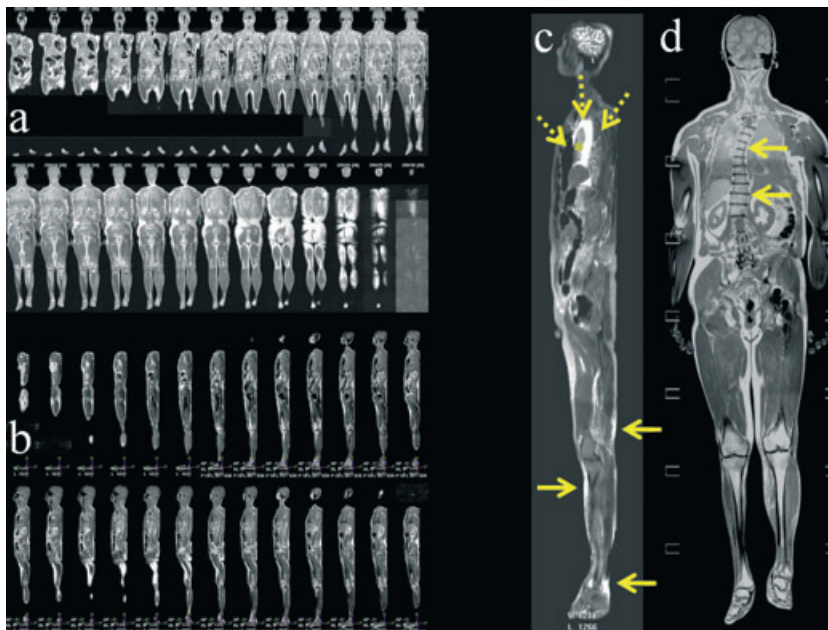


FIG. 5—Whole-body postmortem magnetic resonance imaging for soft tissue documentation in a case of a vehicle accident as driver. (a + b) Exemplarily shown are a coronal (upper) and sagittal (lower) slice stack in T1 weighting each. (c) Sagittal T2-weighted image. Dashed arrows indicate hemothorax with typical layering of air, serum, and erythrocytes. Asterisk indicates collapsed lung floating within the serum layer. Arrows indicate several subcutaneous hematoma at the lower legs. (d) Coronal T1-weighted example image providing excellent anatomic overview. Arrows indicate severe scoliosis.

relations. The reddish distribution of the hematoma between skull bone and skin and along the wound channel as well as the sub-arachnoidal bleedings are clearly demonstrated in their 3D distribution.

*Whole-body Imaging*

Figure 5 shows a set of coronal and sagittal whole corpse images in T1 and T2 weighting in a case of a motor vehicle accident. The T2-weighted images document all subcutaneous and fracture-related hematomas in scale, which can be used for reconstruction purposes. The left-sided hematonpneumothorax as the cause of death is best seen on the sagittal T2-weighted images.

**Discussion**

The present publication exemplarily demonstrates that MR data of a corpse can be acquired and stored in a way that enables sophisticated postprocessing optimized for any purpose. Investigations into digital body data can be performed even years after the corpse has been buried and newly arising questions concerning soft tissue findings can be addressed in a specifically optimized manner. CT has already provided this opportunity for skeletal findings and for gas accumulations within the body in a forensically satisfying quality, and MR imaging can now catch up with extending this objective to an in-scale 3D documentation of all soft tissues of the corpse as well (Table 1). Thereby the absence of, e.g., a myocardial infarction can be proven if necessary or its localization and dimensions can be assessed and visualized (16).

*What Will be the Intermediate-term Impact on Postmortem Investigations?*

Especially, the quantified MR data open new horizons for the use of MR imaging. As the normal relaxation behavior of any tissue can now be expressed in a specific tissue value given by a combination of T1, T2, and PD values, any alterations can be assessed by quantifying their relaxation behavior. Having established and validated certain ranges for normal tissue and its pathological alterations, automatic image analysis will become possible. Initial studies (including postmortem studies) are already in progress to create a feasible scale to work with for human tissue quantification data. After validation, there will be a MR quantification scale comparable to the Hounsfield Unit scale in CT, but with a distinctively more powerful soft tissue analysis potential.

However, as the signal behavior of tissues in MR is much more sensitive than X-ray absorption behavior in CT, the MR values are distinctively more susceptible to varying characteristics of the corpse. Especially, the strong temperature dependence of predominantly the T1 relaxation time needs to be taken into consideration when compiling tissue ranges as these will be only valid for a known body temperature. A possible solution for that problem is provided by the introduced approach itself based on the strong temperature dependence of the T1 relaxation. When the temperature–T1 relaxation time curve is obtained for tissues that are relatively stable in composition, such as cerebrospinal fluid or the serum layer in sedimented blood, these curves can be consulted to estimate the body core temperature the corpse had during scanning. First, feasibility *ex situ* experiments on the temperature dependence of human serum turned out to be promising and justify future validation studies to be performed. By having the quantified MR data of a corpse, the accuracy of MR-based temperature estimation may be improved by combining temperature curves of several relatively stable composed tissues.

The strong dependence of the technique on the hydrogen protons of water may become a problem to solve when compiling normal tissue ranges as, e.g., in open trauma cases the drying of internal tissues can affect the obtained tissue values. As an example, one of the first examined corpses presented with an open trauma to the skull and the brain values behaved distinctively different from further examined cases. On the other hand, it may become a very sensitive technique to quantify the water content of tissues. In other words, edematous tissue alterations can be quantified objectively by measuring the water content and by correlating the obtained values to normal ranges. This possibility will open up horizons in future cerebral and myocardial diagnostics.

Besides having also the entire soft tissue of the human body documented in a nonobserver-dependent manner and in 3D, which is an enormous advance in itself, the quantified nature of the data set gives new and very promising tools to work with. Knowing the pmMR relaxation behavior of, e.g., inflammatory processes, it will be possible to check the whole corpse for an inflammation within seconds by searching for voxels that show an inflammatory-specific combination of T1 and T2 relaxation times and PD highlighted by a certain color encoding. Knowing the specific relaxation behavior of different tumors, the data enable checking the corpse for a possible metastasis distribution within seconds and in a spatial resolution that no autopsy can reach. Based on the results from a recent study (25), this already became true for hemorrhages, which is indicated in Fig. 4. The list may be extended with all the soft tissue findings

TABLE 1—Comparison of strengths and weaknesses of computed tomography (CT), clinical MRI, and IQpmMR. The application of CT and IQpmMR in a combined manner represents the optimal whole-body documentation approach for forensic purposes (bold print).

	CT	Clinical MRI	IQpmMR
A—Skeleton, dentition, foreign bodies, gaseous findings—visualization in 2D	Excellent	Poor–moderate	Moderate
B—General soft tissue visualization in 2D	Poor–moderate	Excellent	Excellent
C—Reformatting	Excellent	Poor	Excellent
D—Volume rendering	Excellent	Poor	Excellent
E—Quantitative tissue characterization (skeleton, dentition, foreign bodies, gas)	Excellent (partly extended Hounsfield Unit scale)	Poor	Moderate (3D-T1, T2, PD-space)
F—Quantitative tissue characterization (soft tissue anatomy and pathology)	Moderate (Hounsfield Unit scale)	Moderate	Excellent (3D-T1, T2, PD-space)
<b>G—Color encoded 3D tissue visualization (D + E)</b>	<b>Excellent</b>	Poor	<b>Moderate</b>
<b>H—Color encoded 3D tissue visualization (D + F)</b>	<b>Moderate</b>	Poor	<b>Excellent</b>

MRI, magnetic resonance imaging; IQpmMR, isotropic and quantified postmortem magnetic resonance.

that are relevant in postmortem examinations and which contain sufficient tissue hydrogen protons to work with. Even in severely putrefied corpses, pmMRI can still provide pathological insight into, e.g., the brain when autopsy already fails in dissecting the organ as a consequence of the liquidation. Therefore, the technique may be of limited value only in severely mummified corpses (26) or in adipocere cases (27).

The data acquisition technique that fulfills the requirements of sufficient soft tissue documentation could already be implemented. Today's shortcoming of the introduced technique is that there is no software, which combines all visualization possibilities that the acquired data provide. Reformatting and volume rendering run well on regular radiological workstations. For generating synthetic MR images, the data need to be loaded onto a personal computer with software recently developed for that purpose. At the time of manuscript submission, a first plug-in for a Picture Archiving and Communication System is about to be implemented but it is not implemented yet on radiological workstations in a general manner. Therefore, the current research efforts at the publication's host institutes aim on implementing a forensically optimized workstation for postmortem CT and MR data sets (28). For the suitable use of IQpmMR data, the workstation should allow reformatting, volume rendering, and change of contrast weighting in quantified isotropic MR data sets of a whole corpse to be handled. Computer-aided diagnostics need to be implemented based on established ranges of the signal behavior of normal postmortem tissue and pathological alterations. Besides automated localization of pathological soft tissue findings, a volumetric quantification might also be performed automatically, e.g., the blood volume contained in subcutaneous and internal hematoma may be calculated and can thereby be related to the cause of death as well.

For MR scanning, the main issue that needs to be taken into consideration is the scanning time. All the given study example cases were scanned within a time frame of 1.5 h. These scans consisted of a whole-body scanning using a proper T1 and T2 weighting in sagittal and coronal planes, which took *c.* 20 min. Additionally, the head and neck or the thorax were documented using IQpmMR, which took another *c.* 60 min. The remaining 10 min were used for corpse and coil handling as well as for localizer scanning. The acquired data sets have a size of *c.* 1 gigabyte.

Within a reasonable examination time frame of 2 h, a whole corpse can be documented using the IQpmMR technique in a spatial resolution of *c.* 1.5 mm (depending on the actual length of the body) on today's most spread 1.5 tesla scanners. For future applications using 3 tesla scanners, the spatial resolution of 1.2 mm as given in the example data sets can be extended to the entire corpse not exceeding 2 h of scan time.

## Conclusion

The present work introduces the methodological progress that optimizes MR scanning for the forensic environment and for post-mortem use in general. The MR data are acquired in a quantified manner, which allows for any known noncontrast agent-enhanced image weighting to be synthetically calculated. Furthermore, the data are provided in sufficient isotropic spatial resolution that enables sophisticated 3D postprocessing, such as reformatting any wanted image plane or volume rendering, to display the entire 3D whole volume. Quantification in isotropic resolution allows characterization and color encoding of tissues and pathologies in 3D imaging. The whole body can be documented from head to toe by MRI. Therefore, the combination of the introduced approaches has the potential to catch up to the application of CT by

providing the missing soft tissue information in a comparably complete way.

## Acknowledgments

The authors express their gratitude to Lotta Nordén-Petersson (Department for Forensic Medicine, RMV, Linköping) for the reliable support in case management as well as to Elisabeth Wålin, Peggy Florhed-Hermansson, Ann-Charlotte Skiölt, and Nobar Ashjian (Department for Forensic Medicine, RMV, Linköping) for their experienced assistance at autopsy and their support in logistic aspects of the study. Furthermore, we thank the team of forensic examiners at the Department for Forensic Medicine in Linköping for varying contributions that enabled the research performed for the present work.

## References

1. Poulsen K, Simonsen J. Computed tomography as routine in connection with medico-legal autopsies. *Forensic Sci Int* 2007;171(2-3):190-7.
2. Levy AD, Harcke HT, Getz JM, Mallak CT, Caruso JL, Pearce L, et al. Virtual autopsy: two- and three-dimensional multidetector CT findings in drowning with autopsy comparison. *Radiology* 2007;243(3): 862-8.
3. Shiotani S, Kohno M, Ohashi N, Yamazaki K, Nakayama H, Watanabe K, et al. Non-traumatic postmortem computed tomographic (PMCT) findings of the lung. *Forensic Sci Int* 2004;139(1):39-48.
4. Dirnhofer R, Jackowski C, Vock P, Potter K, Thali MJ. VIRTOPSY: minimally invasive, imaging-guided virtual autopsy. *Radiographics* 2006;26(5):1305-33.
5. Thali MJ, Braun M, Buck U, Aghayev E, Jackowski C, Vock P, et al. VIRTOPSY—scientific documentation, reconstruction and animation in forensic: individual and real 3D data based geo-metric approach including optical body/object surface and radiological CT/MRI scanning. *J Forensic Sci* 2005;50(2):428-42.
6. Jackowski C, Aghayev E, Sonnenschein M, Dirnhofer R, Thali MJ. Maximum intensity projection of cranial computed tomography data for dental identification. *Int J Legal Med* 2006;120(3):165-7.
7. Jackowski C, Thali M, Sonnenschein M, Aghayev E, Yen K, Dirnhofer R, et al. Visualization and quantification of air embolism structure by processing postmortem MSCT data. *J Forensic Sci* 2004;49(6):1339-42.
8. Jackowski C, Wyss M, Persson A, Classens M, Thali MJ, Lussi A. Ultra-high-resolution dual-source CT for forensic dental visualization-discrimination of ceramic and composite fillings. *Int J Legal Med* 2008;122(4):301-7.
9. Levy AD, Abbott RM, Mallak CT, Getz JM, Harcke HT, Champion HR, et al. Virtual autopsy: preliminary experience in high-velocity gunshot wound victims. *Radiology* 2006;240(2):522-8.
10. Stein KM, Bahner ML, Merkel J, Ain S, Mattern R. Detection of gunshot residues in routine CTs. *Int J Legal Med* 2000;114(1-2):15-8.
11. Sidler M, Jackowski C, Dirnhofer R, Vock P, Thali M. Use of multislice computed tomography in disaster victim identification—advantages and limitations. *Forensic Sci Int* 2007;169(2-3):118-28.
12. Jackowski C, Sonnenschein M, Thali MJ, Aghayev E, von Allmen G, Yen K, et al. Virtopsy: postmortem minimally invasive angiography using cross section techniques—implementation and preliminary results. *J Forensic Sci* 2005;50(5):1175-86.
13. Jackowski C, Persson A, Thali MJ. Whole body postmortem angiography with a high viscosity contrast agent solution using poly ethylene glycol as contrast agent dissolver. *J Forensic Sci* 2008;53(2):465-8.
14. Patriquin L, Kassirjian A, Barish M, Casserley L, O'Brien M, Andry C, et al. Postmortem whole-body magnetic resonance imaging as an adjunct to autopsy: preliminary clinical experience. *J Magn Reson Imaging* 2001;13(2):277-87.
15. Shiotani S, Yamazaki K, Kikuchi K, Nagata C, Morimoto T, Noguchi Y, et al. Postmortem magnetic resonance imaging (PMMRI) demonstration of reversible injury phase myocardium in a case of sudden death from acute coronary plaque change. *Radiat Med* 2005;23(8):563-5.
16. Jackowski C, Christe A, Sonnenschein M, Aghayev E, Thali MJ. Post-mortem unenhanced magnetic resonance imaging of myocardial infarction in correlation to histological infarction age characterization. *Eur Heart J* 2006;27(20):2459-67.

17. Aghayev E, Yen K, Sonnenschein M, Ozdoba C, Thali M, Jackowski C, et al. Virtopsy post-mortem multi-slice computed tomography (MSCT) and magnetic resonance imaging (MRI) demonstrating descending tonsillar herniation: comparison to clinical studies. *Neuroradiology* 2004;46(7):559–64.
18. Yen K, Sonnenschein M, Thali MJ, Ozdoba C, Weis J, Zwiygart K, et al. Postmortem multislice computed tomography and magnetic resonance imaging of odontoid fractures, atlantoaxial distractions and ascending medullary edema. *Int J Legal Med* 2005;119(3):129–36.
19. Haacke ME, Brown RW, Thompson MR, Venkatesh N. *Magnetic resonance imaging—physical principles and sequence design*, 1st edn. New York, NY: John Wiley & Sons, 1999.
20. Warntjes JB, Leinhard OD, West J, Lundberg P. Rapid magnetic resonance quantification on the brain: optimization for clinical usage. *Magn Reson Med* 2008;60(2):320–9.
21. Warntjes JB, Dahlqvist O, Lundberg P. Novel method for rapid, simultaneous T1, T\*2, and proton density quantification. *Magn Reson Med* 2007;57(3):528–37.
22. Riederer SJ, Lee JN, Farzaneh F, Wang HZ, Wright RC. Magnetic resonance image synthesis. Clinical implementation. *Acta Radiol Suppl* 1986;369:466–8.
23. Bobman SA, Riederer SJ, Lee JN, Suddarth SA, Wang HZ, Drayer BP, et al. Cerebral magnetic resonance image synthesis. *AJNR Am J Neuroradiol* 1985;6(2):265–9.
24. Zhu XP, Hutchinson CE, Hawnaur JM, Cootes TF, Taylor CJ, Isherwood I. Magnetic resonance image synthesis using a flexible model. *Br J Radiol* 1994;67(802):976–82.
25. Jackowski C, Thali M, Aghayev E, Yen K, Sonnenschein M, Zwiygart K, et al. Postmortem imaging of blood and its characteristics using MSCT and MRI. *Int J Legal Med* 2006;120(4):233–40.
26. Jackowski C, Bolliger S, Thali M. Scenes from the past—common and unexpected findings in mummies from Ancient Egypt and South America revealed by CT. *Radiographics* 2008;28(5):1477–92.
27. Jackowski C, Thali M, Sonnenschein M, Aghayev E, Yen K, Dirnhofer R. Adipocere in postmortem imaging using multislice computed tomography (MSCT) and magnetic resonance imaging (MRI). *Am J Forensic Med Pathol* 2005;26(4):360–4.
28. Ljung P, Winskog C, Persson A, Lundstrom C, Ynnerman A. Full body virtual autopsies using a state-of-the-art volume rendering pipeline. *IEEE Trans Vis Comput Graph* 2006;12(5):869–76.

Additional information and reprint requests:  
 Christian Jackowski, M.D.  
 Institute of Legal Medicine  
 University of Zürich  
 Winterthurerstrasse 190/52  
 8057 Zürich  
 Switzerland  
 E-mail: christian.jackowski@irm.uzh.ch